Research Square

Preprints are preliminary reports that have not undergone peer review.
They should not be considered conclusive, used to inform clinical practice,
or referenced by the media as validated information.

Engineering Verification and Quality Evaluation of Underground Concrete Slipform Paving with Accelerator- Incorporated Side Support

Cheng Wang
Zaozhuang Mining Group Jiang'zhuang Coal Industry Co., Ltd
Yongjing Deng
Shandong University of Science and Technology
Yutao Zhang
m17852601969@163.com

Shandong University of Science and Technology

Article

Keywords: slipform paving, concrete containing accelerator, speed parameter optimization, discrete element method (DEM), process adaptability, underground floor

Posted Date: September 16th, 2026

DOI: https://doi.org/10.21203/rs.3.rs-10746427/v1

License: This work is licensed under a Creative Commons Attribution 4.0 International License.
Read Full License

Additional Declarations: No competing interests reported.

Engineering Verification and Quality Evaluation of Underground Concrete Slipform Paving with Accelerator-Incorporated Side Support

Cheng Wang [a] ;Yongjing Deng [b] ; Yutao Zhang [b,*]

a, Zaozhuang Mining Group Jiang'zhuang Coal Industry Co., Ltd

Zaozhuang，shandong，277800，China

b, School of Safety and Environmental Engineering, Shandong University of Science and Technology, Qingdao, Shandong 266590

* Corresponding author

E-mail: m17852601969@163.com, Tel:+86 1785-260-1969 (Yutao Zhang)

Abstract: In the slipform paving of underground roadway floors, the abrupt dissipation of lateral constraints post-extrusion frequently induces edge collapse, structural deformation, and lateral displacement. To mitigate these challenges, this study proposes a novel composite slipform paving strategy characterized by the localized application of an alkali-free liquid accelerator to the bilateral strips, while the central section is cast with conventional concrete. Field validation was conducted in an underground coal mine utilizing optimized operational parameters: a 9% dosage of FSA-AF alkali-free liquid accelerator, a 14 cm width for the accelerator-modified side zones, an auger rotation speed of 45 r/min, and a paving velocity of 6.0 m/min. The morphological stability, surface flatness, and mechanical properties of the paved floor were systematically evaluated through in-situ testing. The results demonstrate that the proposed composite paving process effectively eliminates observable edge collapse, cracking, and displacement, with the average lateral deformation restricted to merely 1 mm, thereby satisfying rigorous engineering tolerances. Based on the 3-meter straightedge method, the average surface flatness was recorded at 4.6 ± 0.2 mm. Furthermore, 3D imaging analysis revealed average flatness values of 4.1 mm and 2.8 mm for the side and central segments, respectively, corresponding to "relatively high" and "high" flatness grades. Regarding mechanical integrity, the side concrete achieved average compressive and flexural strengths of 33.925

MPa and 4.151 MPa, respectively, while the central concrete exhibited superior values of 43.637 MPa and 4.925 MPa. All mechanical indices met the requisite engineering standards. This research confirms that enhancing the "standing performance" of edges through localized acceleration, coupled with optimized kinematic parameters, facilitates high-quality, continuous slipform paving. This methodology provides a robust technical framework for the mechanized and efficient construction of mine roadway floors.

Keywords: slipform paving; concrete containing accelerator; speed parameter optimization; discrete element method (DEM); process adaptability; underground floor.

1. Introduction

The roadway floor serves as a critical structural foundation for underground transportation and operational systems in coal mines. Its service condition directly affects vehicle traffic safety, transportation efficiency, and the environments for subsequent equipment installation and maintenance [1-7]. Historically, concrete paving for underground roadway floors has predominantly relied on manual formwork, paving, and leveling. These conventional methods are characterized by high labor intensity and low construction efficiency. Moreover, the forming quality is significantly influenced by on-site working conditions and human experience, struggling to meet the modern coal mine development goals of "mechanized substitution, automated reduction, and intelligent unmanned operations" [1, 7-13]. Consequently, replacing traditional manual processes with mining slipform paving equipment has emerged as a crucial development direction for underground floor construction technologies [8-17].

Compared to surface roads and conventional municipal pavements, the construction environment for underground roadway floors is significantly more complex. Factors such as narrow roadway spaces, uneven base surfaces, and limited on-site drainage and ventilation conditions adversely affect the stability of the slipform paving process [2-7]. Particularly at the moment of concrete extrusion, the lateral constraints from the formwork rapidly disappear. If the fresh concrete lacks sufficient early standing performance, it is highly susceptible to edge collapse, deformation, and lateral displacement, which consequently compromises the overall forming quality of the floor [8-18]. Existing research on slipform paving primarily focuses on surface applications such as highways, shoulders, curbs, and barriers. These studies emphasize the optimization of material workability, the design of low-slump concrete, equipment and process control, and surface quality evaluation [8-27]. It is generally concluded that an appropriate water-cement ratio, excellent workability of fresh concrete, rapid early strength development, and a construction process system well-coordinated with equipment parameters are critical factors for ensuring slipform paving quality [14-27].

Regarding the regulation of admixtures, accelerators are widely utilized in shotcrete and rapid repair material systems due to their ability to significantly shorten setting times

and accelerate early structural buildup [28-35]. Previous studies have demonstrated that alkali-free liquid accelerators offer distinct advantages in improving early setting, promoting hydration reactions, and enhancing rapid forming capabilities. However, an excessive dosage may adversely affect the long-term strength of the concrete [28-35]. This implies that introducing accelerators into the slipform paving process could provide a novel approach to resolving the issue of insufficient lateral standing performance; however, its impacts on surface quality and long-term mechanical properties must be simultaneously carefully considered.

Building upon this premise, this paper proposes a novel composite slipform paving concept for underground floors, characterized by "accelerator-incorporated concrete on the sides and conventional concrete in the center." Specifically, while ensuring the long-term structural performance of the central load-bearing concrete, an alkali-free liquid accelerator is applied to the bilateral zones. This rapidly enhances the setting and standing capabilities of the side concrete, thereby mitigating edge collapse, deformation, and lateral displacement. While previous research has optimized the type and dosage of the accelerator, the water-cement ratio, lateral dimensional parameters, and equipment operational speeds, this study advances the work by conducting an engineering validation in an actual underground setting. The engineering performance of the proposed method is systematically evaluated in terms of overall forming quality, surface quality and flatness, as well as compressive and flexural mechanical properties. The findings of this study aim to provide valuable references for the broader application of underground slipform paving equipment and the determination of optimal process parameters.



Figure.1 Experimental study on sliding mode paving of concrete roadway floor

2. Materials and Methods

2.1 Technical Route

The core objective of the engineering experiments in this study is to verify the applicability and reliability of the previously determined material parameters, dimensional parameters, and equipment operational parameters under actual underground working conditions. Considering that the engineering acceptance of roadway floors not only evaluates the overall shape quality immediately after extrusion but also requires the floor to withstand the repeated impacts of high-frequency, heavy-duty vehicles and mechanical equipment during long-term service, this study conducts engineering validation across the following three dimensions:

(1) Overall forming quality validation: This focuses on observing whether edge collapse, deformation, or lateral displacement occurs on the sides of the floor post-extrusion, thereby verifying the standing performance of the accelerator-incorporated concrete on the edges and the rationality of the side-width parameters.

(2) Surface quality validation: Visual inspection, the 3-meter straightedge method, and 3D imaging techniques are comprehensively employed to evaluate the apparent quality and flatness of the floor. The analysis specifically focuses on the impact of the accelerator on the surface quality of the side edges.

(3) Mechanical properties validation: The compressive and flexural strengths of the concrete in both the side and central sections are tested to assess whether this composite slipform paved floor retains sufficient long-term load-bearing capacity while fulfilling the requirement for rapid forming.

2.2 Key Process Parameters

The parameters utilized in the engineering tests were all derived from the optimized results of our previous research. The main body of the concrete employed an optimized low water-cement ratio paving mix design, with a water-cement ratio of 0.4. The side regions utilized an FSA-AF alkali-free liquid accelerator at a dosage of 9%. The design width of the accelerator-incorporated concrete on the sides was set to 14 cm. For the

slipform paving machine, the auger shaft rotation speed was set to 45 r/min, and the forward speed of the entire machine was maintained at 6.0 m/min. The aforementioned parameters correspond, respectively, to the requirements for rapid material forming, lateral stability, and the synchronization between equipment material supply and spreading. They represent the optimal combination jointly determined through prior theoretical analyses, single-factor experiments, orthogonal optimization experiments, and Discrete Element Method (DEM) simulations [16, 21, 28-35].

2.3 Engineering Implementation Process

To improve on-site construction efficiency and ensure the accuracy of the concrete mix proportions, the concrete used for paving the floor was uniformly mixed at a centralized batching plant and subsequently transported to the site. Prior to formal paving, the spraying speed and flow rate of the accelerator spray pump were initially calibrated. This ensured that the dosage and mixing uniformity of the accelerator in the lateral concrete strictly met the design requirements. Subsequently, the trailing formwork of the slipform paving machine was adjusted to guarantee that the overall forming width and side dimensions aligned with the previously optimized results. Following this, trial runs were conducted to calibrate the auger shaft rotation speed and the machine's forward speed. This step confirmed that the equipment operating parameters met the predetermined set values and ensured a highly coordinated match between the auger material distribution and the forward movement of the machine. Once the comprehensive calibration of all parameters was completed, the actual continuous slipform paving of the roadway floor was executed.



Figure.2 Concrete preparation and cutting process



Figure.3 Debugging of accelerators spray pump.



Figure.4 Spiral shaft speed debugging and test drive



Figure.5 Experimental study on sliding mode paving of concrete roadway floor

2.4 Quality Evaluation Methods

2.4.1 Overall Forming Quality Evaluation

The overall forming quality primarily encompasses three aspects: edge collapse, deformation, and lateral displacement. Edge collapse was assessed through visual

inspection and on-site photography. Deformation was measured using a dual-laser rangefinder method, where laser rangefinders were positioned at the upper and lower locations of the same vertical reference base. The difference in distance from the rangefinders to the top and bottom of the lateral concrete was recorded to represent the lateral deformation. Lateral displacement was determined by comparing the width of the paving machine's trailing formwork with the actual width of the paved floor. If the two values were consistent, it was considered that no obvious lateral displacement had occurred.

2.4.2 Surface Quality and Flatness Evaluation

The surface quality of the floor was initially evaluated via visual inspection to determine the presence of macro-defects such as pitting, holes, and depressions in both the lateral and central regions. Subsequently, the 3-meter straightedge method was employed to measure the maximum gap on the floor surface, thereby evaluating its macroscopic flatness. Considering the relatively low early strength of the concrete surface during the initial setting stage, the inherent weight of the 3-meter straightedge and wedge feeler gauge could potentially interfere with the measurement results. Therefore, a Leica-DVM 5000-HD 3D imager was further introduced to conduct 2D/3D imaging analysis on the surfaces of the cut test blocks. The surface flatness was characterized by the elevation difference between the highest and lowest points, providing a more precise evaluation.

2.4.3 Mechanical Properties Evaluation

A universal testing machine was utilized to determine the compressive and flexural strengths of the concrete specimens obtained from the lateral and central sections of the floor. The compressive specimens were prepared from blocks cut directly from the site, while the flexural specimens were obtained through on-site sampling, molding, and subsequent standard curing. By comparing the mechanical property differences between the concrete in these two regions, the impact of the accelerator on long-term strength was analyzed, and the capability of the composite slipform paved structure to meet the long-term service requirements of underground floors was evaluated.

3. Results and Discussion

3.1 Overall Forming Quality of the Floor

3.1.1 Edge Collapse Control Effect

Following the completion of the on-site slipform paving, the forming status of both sides of the floor was directly observed. The results indicated no obvious collapse, cracking, or large-scale flow in the lateral regions. This demonstrates that the accelerator-incorporated lateral concrete can rapidly establish sufficient early structure upon extrusion, satisfying the engineering requirements of "rapid setting, low slump, and no edge collapse." This finding confirms that selectively applying the accelerator to the lateral regions, rather than uniformly mixing it into the entire concrete batch, is a viable approach to solving the edge instability problem in underground slipform paving. On the one hand, this method effectively enhances the standing performance of the edge regions; on the other hand, it preserves the long-term load-bearing capacity of the central conventional concrete to the greatest extent possible. This strategy significantly differs from the traditional approaches of globally reducing the slump or uniformly increasing the accelerator dosage [18-21, 28-35].



Figure.6 Detection of collapsed edges in side concrete

3.1.2 Lateral Deformation Characteristics

The lateral deformation was further quantified using the dual-laser rangefinder method. The differences recorded at three measurement points were 0.001 m, 0 m, and 0.002 m, respectively, resulting in an average deformation of 0.001 m (i.e., 1 mm). This

value is clearly within the permissible engineering tolerance. The results indicate that with a 9% accelerator dosage and a 14 cm lateral width parameter, the side concrete maintains excellent geometric stability after extrusion, without obvious lateral bulging or top collapse. This is attributable both to the accelerator's role in promoting early structural formation and to the adequacy of the previously determined lateral dimensional parameters in providing sufficient stability reserves for the edge zones.



Figure.7 Detection of deformation problems in side concrete

Table 1. Deformation detection results of side concrete

Point ID	Distance to Top Edge (m)	Distance to Bottom Edge (m)	Difference (m)	Mean Value (m)
Point 1	0.468 m	0.469 m	0.001 m	0.001 m（1 mm）
Point 2	0.461 m	0.461 m	0 m	
Point 3	0.471 m	0.473 m	0.002 m	

3.1.3 Displacement Control Effect

A comparison between the width of the slipform paving machine's trailing formwork and the overall width of the formed floor revealed that both measurements were 310 cm. The consistency of the dimensions before and after paving indicates that no obvious lateral displacement occurred during construction. In other words, with a 14 cm width of accelerator-incorporated concrete, the lateral regions not only possess sufficient deformation resistance but also maintain geometric boundary stability against the lateral pressure exerted by the central concrete, preventing outward expansion. This further corroborates the theoretical design and experimental validation of the lateral width parameter in an actual engineering setting.

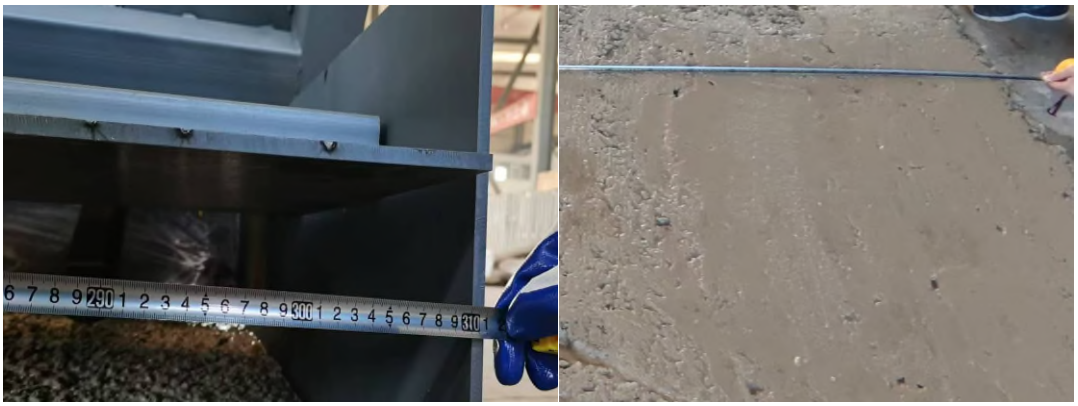


Figure.8 Detection of displacement problem of side concrete

In summary, adopting the slipform paving process with accelerator-incorporated lateral support yields excellent overall forming quality for the floor, effectively suppressing edge collapse, deformation, and displacement. This demonstrates a strong engineering compatibility among the material parameters, lateral dimensional parameters, and equipment operational parameters.

3.2 Surface Quality and Flatness Evaluation

3.2.1 Apparent Defect Analysis

Photographic and visual analyses of local areas in the lateral and central regions of the floor revealed no obvious macroscopic defects such as pitting, holes, or depressions. This suggests that despite the addition of the accelerator in the lateral zones, the overall surface quality did not deteriorate significantly due to localized rapid setting. From a macroscopic perspective, the entire floor surface is continuous and dense, satisfying the basic visual requirements for underground roadway structures.



Figure.9 Local situation of side concrete (left) and middle concrete (right)

3.2.2 Flatness by 3-Meter Straightedge Method

The surface flatness of the floor measured by the 3-meter straightedge method at three different points was 4.4 mm, 4.8 mm, and 4.5 mm, yielding an average of 4.6 mm. These results indicate that the paved floor in the engineering trial not only meets general flatness requirements but also approaches a relatively high flatness standard. For underground roadway floors, superior flatness translates to reduced vehicle vibration, improved tire-floor contact, and a decrease in localized impact loads and future maintenance pressures. Thus, these findings highlight the high practical engineering value of the optimized process parameters.



Figure.10 Three meters straightedge method for measuring surface flatness

Table 2. Measurement results using the three meters straightedge method

Point 1	Point 2	Point 3	Average
4.4 mm	4.8 mm	4.5 mm	4.6 mm

Because the 3-meter straightedge method is conducted during the early stages post-extrusion, the weight of the testing tool itself may cause slight indentations on the incompletely hardened surface. Consequently, its results primarily serve as a rapid macroscopic evaluation rather than reflecting the true geometric surface state after final setting. To accurately evaluate the surface quality of different regions, supplementary analysis using 3D imaging is necessary.

3.2.3 Fine Evaluation by 3D Imaging Method

Locations with the maximum gaps identified by the 3-meter straightedge were marked and cored. After standard curing, 3D surface imaging analysis was conducted using the Leica-DVM 5000-HD. The elevation differences at three lateral measurement points were 4031.0 μm, 4308.7 μm, and 4031.0 μm, respectively, whereas those at three central measurement points were 2933.1 μm, 2467.2 μm, and 3014.3 μm. Statistical analysis revealed an average flatness of 4.1 mm for the lateral regions and 2.8 mm for the central region. Both regions exhibited excellent flatness, with the central concrete surface being superior.

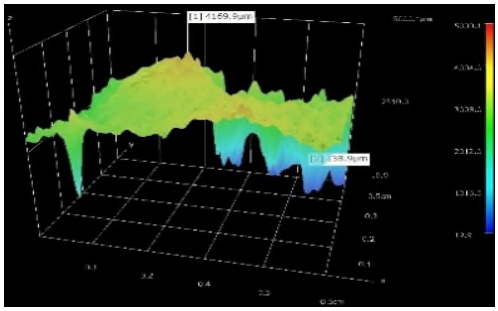
The slightly lower flatness in the lateral regions compared to the central region may be attributed to the rapid surface setting promoted by the accelerator. Specifically, after the lateral concrete is extruded and smoothed by the trailing formwork, its surface enters the setting phase more quickly, thereby diminishing subsequent subtle self-leveling and reshaping capabilities. Simultaneously, localized rapid hydration may cause the surface to solidify earlier, locking in minor micropores and microscopic undulations. In contrast, the setting process of the central conventional concrete is relatively slower, allowing the extrusion and smoothing action of the formwork to be fully realized, thus producing a smoother surface. Nevertheless, an average flatness of 4.1 mm in the lateral regions still represents a high standard, while the 2.8 mm in the center reaches a premium standard, indicating that the localized use of the accelerator does not lead to unacceptable compromises in surface quality.



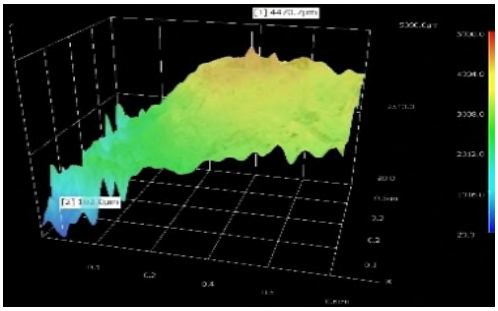
Figure.11 Determination of the maximum gap position (left) and sampling of concrete test blocks (right)



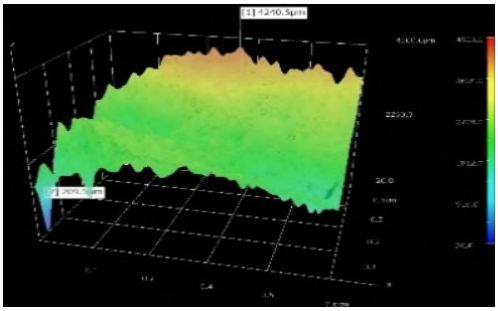
Figure.12 Test block maintenance (left) and 3D imaging experiment process (right)



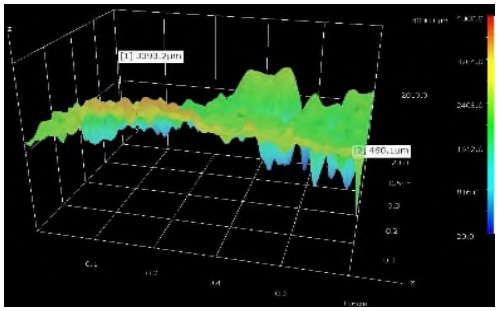
(a) Lateral Measuring Point 1



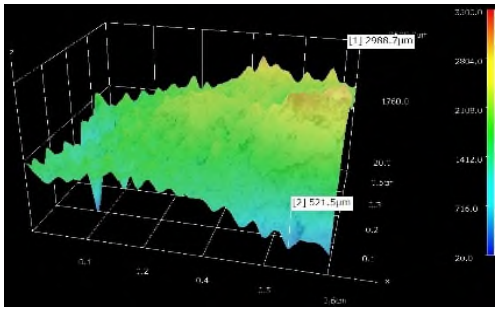
(b) Lateral Measuring Point 2



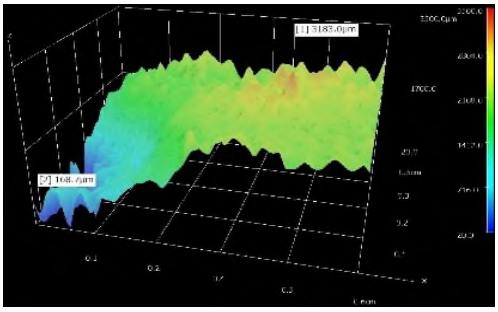
(c) Lateral Measuring Point 3



(d) Central Measuring Point 1



(e) Central Measuring Point 2



(f) Central Measuring Point 3

Figure.13 3D imaging of the surface of concrete bottom plate

Table 3. Flatness detection results of 3D imaging method

3D Imaging Position	Lateral Measuring Point 1	Lateral Measuring Point 2	Lateral Measuring Point 3	Central Measuring Point 1	Central Measuring Point 2	Central Measuring Point 3
Maximum Value（μm）	4169.9	4470.7	4240.5	3393.2	2988.7	3183.0
Minimum Value（μm）	138.9	162.0	209.5	460.1	521.5	168.7
Difference（μm）	4031.0	4308.7	4031.0	2933.1	2467.2	3014.3
Average Value（mm）		4.1			2.8	

3.3 Mechanical Properties Evaluation

Following the successful on-site verification of the overall shape and surface quality, the compressive and flexural strengths of the concrete in both regions were tested. The compressive strengths of three lateral specimens were 34.114 MPa, 32.581 MPa, and 35.079 MPa, averaging 33.925 MPa; their flexural strengths were 4.186 MPa, 4.239 MPa, and 4.028 MPa, averaging 4.151 MPa. For the central concrete, the compressive strengths of three specimens were 44.682 MPa, 44.965 MPa, and 41.264 MPa, averaging 43.637 MPa; the flexural strengths were 4.912 MPa, 4.954 MPa, and 4.909 MPa, averaging 4.925 MPa.



Figure.14 Mechanical performance testing of concrete roadway floor

Table 4. Test results of compressive and flexural strength

Test Position	Test Index（MPa）	Sample 1	Sample 2	Sample 3	Average Value
Lateral Concrete	Compressive Strength	34.114	32.581	35.079	33.925
	Flexural Strength	4.186	4.239	4.028	4.151
Central Concrete	Compressive Strength	44.682	44.965	41.264	43.637
	Flexural Strength	4.912	4.954	4.909	4.925

Evidently, both the compressive and flexural strengths of the lateral accelerator-incorporated concrete are lower than those of the central conventional concrete. This trend aligns with the established understanding that high accelerator dosages can impair long-term strength development [28-35]. The underlying reason is that while accelerators significantly accelerate early setting and structural formation, high dosages may alter the hydration trajectory and pore structure evolution of the cementitious system, adversely affecting long-term strength. However, the most critical finding of this study is that despite a certain degree of strength reduction in the lateral regions, their absolute compressive and flexural strengths remain substantial. Combined with the central region, the overall composite floor structure fully satisfies the basic load-bearing requirements for underground roadways.

This suggests that for underground slipform paving, the composite structural concept of "rapid forming on both sides and main load-bearing in the center" is highly rational. The primary function of the lateral regions is rapid standing and boundary stabilization, with load-sharing as a secondary role; the central conventional concrete assumes the primary long-term load-bearing responsibility. Therefore, accepting a moderate reduction in long-term strength in the lateral zones as a trade-off for significantly enhanced extrusion stability and overall construction quality is an engineering-validated parameter optimization strategy.

3.4 Engineering Significance and Method Applicability Analysis

This study demonstrates that the quality of underground slipform paving is not governed by material, structure, or equipment factors in isolation, but by their coupled effects. Materially, the alkali-free liquid accelerator endows the lateral regions with sufficiently rapid early setting and standing capabilities. Structurally, the 14 cm lateral width provides the necessary stable geometric conditions for the edges. Equipment-wise, the auger shaft rotation speed of 45 r/min and the forward speed of 6.0 m/min ensure uniform material distribution and continuous forming. The synergistic action of these three factors ultimately achieves excellent engineering results.

Compared to traditional methods that solely rely on lowering slump or globally increasing concrete "stiffness," the localized rapid-setting support concept proposed in this study is more targeted. Its advantages lie in effectively mitigating edge instability while avoiding the detrimental effects of high global accelerator dosages on the long-term performance of the main concrete body. Furthermore, this process exhibits high compatibility with the existing sequence of spraying pump–auger distribution–trailing formwork extrusion in current slipform paving machines, showing significant potential for widespread application.

Admittedly, this paper primarily focuses on a single engineering validation trial. More systematic research is required regarding varying roadway gradients, fluctuating base conditions, and long-term service durability. Future work should delve into field adaptability under multiple working conditions, repetitive construction stability, and long-term wear-fatigue performance.

4. Conclusions

1. Based on previously optimized parameters for materials, lateral dimensions, and equipment speeds, stable slipform paving of underground roadway floors can be successfully achieved using an FSA-AF alkali-free liquid accelerator at a 9% dosage, a 14 cm lateral width, and a speed combination of 45 r/min (auger) to 6.0 m/min (forward movement).

2. Engineering trials verify that implementing accelerator-incorporated lateral support prevents obvious edge collapse. The average lateral deformation is strictly limited to 1 mm, and the formed floor width strictly aligns with the formwork width, indicating that this method effectively suppresses edge collapse, deformation, and displacement during slipform paving.

3. The overall surface quality of the paved floor is excellent. The average flatness measured by the 3-meter straightedge method is 4.6 mm. 3D imaging results show average flatness values of 4.1 mm and 2.8 mm for the lateral and central regions, respectively. Although the lateral flatness is slightly lower due to the rapid-setting effect, both regions exhibit superior surface quality levels.

4. The average compressive and flexural strengths of the lateral accelerator-incorporated concrete are 33.925 MPa and 4.151 MPa, respectively, while those of the central conventional concrete are 43.637 MPa and 4.925 MPa. Despite the lower long-term strength in the lateral regions, both sections fulfill engineering application requirements, demonstrating that the composite slipform paved floor successfully balances rapid forming with long-term load-bearing capacity.

5. Overall, the proposed underground slipform paving method—featuring "accelerator-incorporated concrete on the sides and conventional concrete in the center"—enables high-quality, continuous floor construction. It provides a viable engineering

pathway for the mechanized, continuous, and high-standard development of coal mine roadway floors.

References

[1] B. Yuan, C. A. Li, Z. L. Quan, et al., "Development and application of slipform paver for mine roadway," *China Machinery*, vol. 2023, no. 2, pp. 60-63, 68, 2023. [in Chinese]

[2] M. X. Gao, "Influence of underground pavement conditions on the service performance of trackless vehicles," *Nonferrous Metals (Mining Section)*, no. 4, pp. 12-16, 48, 1994. [in Chinese]

[3] X. M. Chen, "Research on pavement treatment methods of trackless transport roadway in extra-large mines," *Shandong Coal Science and Technology*, no. 1, pp. 134-135, 2013. [in Chinese]

[4] Y. O. Yan, Y. Wu, and Q. Y. Zhang, "Causes and prevention strategies of transport accidents in inclined roadways," *Technology Outlook*, no. 23, p. 214, 2014. [in Chinese]

[5] Y. X. Guo, "Cause analysis of transportation accidents in underground mine roadways," *Information System Engineering*, no. 1, pp. 107-108, 2012. [in Chinese]

[6] J. Geng and Z. X. Lu, "Causes and preventive measures of rail transport accidents in mine shaft roadway construction," *Coal Science & Technology Magazine*, no. 2, pp. 86-88, 2013. [in Chinese]

[7] Z. Fu and H. Li, "Achievement and prospect of cement concrete pavement construction for 30 years in China," *Journal of Highway and Transportation Research and Development*, no. 12, pp. 21-27, 2008. [in Chinese]

[8] D. D. Zhao, "High-quality pavement laying technology based on cement concrete paver," *Construction Machinery*, no. 3, pp. 121-123, 2023. [in Chinese]

[9] Y. K. Hu, "Research on concrete mixture ratio design and slipform paving construction technology of highway curb," *Construction & Design for Project*, no. 11, pp. 187-189, 2023. [in Chinese]

[10] L. Z. Jin, "Application of slipform paving construction technology in cement concrete pavement of expressway," *Construction & Design for Project*, no. 20, pp. 138-140, 2023. [in Chinese]

[11] K. Luo, "Application of slipform paver in highway pavement paving," *Heilongjiang Science and Technology of Communication*, vol. 42, no. 12, pp. 229-230, 2019. [in Chinese]

[12] J. T. Xu, "Large-scale slipform paving construction technology based on low slump concrete concept," *Guangdong Highway Communications*, vol. 45, no. 4, pp. 45-48, 2019.

[in Chinese]
[13] X. M. Ding, "Slipform construction technology for cement concrete pavement," *Heilongjiang Science*, vol. 9, no. 22, pp. 80-81, 2018. [in Chinese]
[14] S. J. Hu, "Research on slipform construction technology of cement concrete pavement," M.S. thesis, *Hebei University of Technology*, 2017. [in Chinese]
[15] D. Z. Ma, "Discussion on slipform paving construction technology of cement concrete pavement," *Shanxi Architecture*, vol. 44, no. 5, pp. 149-151, 2018. [in Chinese]
[16] K. L. Feng, "Research and application of performance of barrier concrete based on slipform paving technology," M.S. thesis, *Beijing Jiaotong University*, 2018. [in Chinese]
[17] R. H. Li, "A full-section slipform paving equipment for UHPC concrete," Chinese Patent CN111827131A, Poly Changda Engineering Co., Ltd., 2020. [in Chinese]
[18] Marllon Daniel Cook, M Tyler Ley, Ashkan Ghaeezadah. A workability test for slip formed concrete pavements[J]. Construction and Building Materials, 2014, 68: 376-383.
[19] Gilson R Lomboy, Kejin Wang, Peter Taylor, et al. Guidelines for design, testing, production and construction of semi-flowable SCC for slip-form paving[J]. International Journal of Pavement Engineering, 2011, 13(3): 216-225.
[20] Kianoush Siamardi, Shahin Shabani, Ahmad Mansourian. Optimization of concrete mixes using mixture approach for slip-formed concrete pavement incorporating blends of limestone aggregates[J]. Construction and Building Materials, 2023, 397: 1-11.
[21] Thomas Voigt, Jean-Juste Mbele J, Kejin Wang, et al. Using Fly Ash, Clay, and Fibers for Simultaneous Improvement of Concrete Green Strength and Consolidatability for Slip-Form Pavement[J]. Journal of Materials in Civil Engineering, 2010, 22(2): 196-206.
[22] Yeo J S, Koting S, Onn C C, et al. Optimisation of mix design of concrete paving block using response surface methodology[J]. Journal of Physics: Conference Series, 2023, 2521: 1-14.
[23] Rakesh Kumar. Influence of recycled coarse aggregate derived from construction and demolition waste (CDW) on abrasion resistance of pavement concrete[J]. Construction and Building Materials, 2017, 142: 248-255.
[24] Cong Ma, Bing Chen. Experimental study on the preparation and properties of a novel foamed concrete based on magnesium phosphate cement[J]. Construction and Building Materials, 2017, 137: 160-168.

[25] Ivana Barišić, Ivanka Netinger Grubeša, Hrvoje Krstić, et al. Field and Laboratory Assessment of Different Concrete Paving Materials Thermal Behavior[J]. Sustainability, 2022, 14(11): 6638-6638.
[26] Abbas Solouki, Piergiorgio Tataranni, Cesare Sangiorgi. Mixture Optimization of Concrete Paving Blocks Containing Waste Silt[J]. Sustainability, 2022, 14(1): 451-451.
[27] Qiqi Tan, Hongzhou Zhu, Song Yang, et al. Precast Assembled Road Paving Technology: Progress and Prospects[J]. Materials, 2024, 17(10): 1-10.
[28] Gang Zhou, Weimin Cheng, Sen Cao. Development of a New Type of Alkali-Free Liquid Accelerator for Wet Shotcrete in Coal Mine and Its Engineering Application[J]. Advances in Materials Science and Engineering, 2015, 2015: 1-14.
[29] Yonghua Su, Biao Luo, Zhengdong Luo, et al. Effect of Accelerators on the Workability, Strength, and Microstructure of Ultra-High-Performance Concrete[J]. Materials, 2021, 15(1): 159-159.
[30] Zhenmin Wan, Tingshu He, Xiaodong Ma, et al. Research on the synergy of micro-nano bubble water and alkali-free liquid accelerator to improve the early strength and hydration rate of cement[J]. Journal of Building Engineering, 2022, 57: 1-15.
[31] Renan P. Salvador, Ignacio Segura, et al. Early age hydration of cement pastes with alkaline and alkali-free accelerators for sprayed concrete[J]. Construction and Building Materials, 2016, 111: 386-398.
[32] Renhe Yang, Tingshu He, Mengqin Guan, et al. Preparation and accelerating mechanism of aluminum sulfate-based alkali-free accelerating additive for sprayed concrete[J]. Construction and Building Materials, 2020, 234: 117334-117334.
[33] Yifei Wang, Lei Lei, Jianhui Liu, et al. Accelerators for normal concrete: A critical review on hydration, microstructure and properties of cement-based materials[J]. Cement and Concrete Composites, 2022, 134: 1-11.
[34] Dashuai Zhang, Xingli Zhang, Haotian Tang, et al. Development of a Novel Type of Liquid Accelerator Based on Aluminum Sulfate and Its Accelerating Mechanism for Cement Hydration[J]. Journal of Materials in Civil Engineering, 2024, 36(1): 04023517-04023517.
[35] Jiahe Wang, Yongjiang Xie, Xinhua Zhong, et al. Test and simulation of cement hydration degree for shotcrete with alkaline and alkali-free accelerators[J]. Cement and

Concrete Composites, 2020, 112: prepublish.

Funding

This research received no external funding.

Data availability

All data generated or analysed during this study are included in this published article.